Electric-field-dependent empirical potentials for molecules and crystals: A first application to flexible water molecule adsorbed in zeolites

P. Cicu, P. Demontis, S. Spanu, G. B. Suffritti, and A. Tilocca
Dipartimento di Chimica, Università di Sassari, Via Vienna 2, I-07100 Sassari, Italy

(Received 13 December 1999; accepted 22 February 2000)

A general method to include electric-field-dependent terms in empirical potential functions representing interatomic interactions is proposed. It is applied to derive an intramolecular potential model for the water molecule able to reproduce the effects of an electric field on its geometry and dynamics: to enlarge the HOH angle, to increase slightly the OH bond lengths, to red-shift the stretching vibrational frequencies, and to blue-shift slightly the bending mode frequency. These effects have been detected experimentally for water adsorbed in zeolites and have been confirmed by quantum mechanical calculations. The electric-field-dependent intramolecular potential model for water has been combined with a newly refined intermolecular potential for bulk water and with new potentials representing cation–water and aluminosilicate–water interactions in order to simulate, by classical molecular dynamics (MD) technique, the behavior of water adsorbed in zeolites. The performances of the model have been checked by a MD simulation of liquid water at room temperature, by the structural and vibrational properties of the water dimer, and by test MD calculations on a hydrated natural zeolite (natrolite). The results are encouraging, and the simulations will be extended to study the behavior of water adsorbed in other zeolites, including diffusion and some aspects of ion exchange processes. © *2000 American Institute of Physics.* [S0021-9606(00)50319-5]

I. INTRODUCTION AND SCOPE

It is well known that molecular dynamics (MD) simulations of atomic and molecular systems[1–3] need for differentiable potential energy functions to solve the equations of motion.

Atoms are made of positively charged nuclei and negatively charged electron clouds which, after chemical bonding or ionization, are deformed or changed and generate variable local electric fields. In condensed state systems, these fields give rise to polarization and more complex effects modifying, in turn, the distribution of charges of the atoms, ions, or molecules.

Therefore, potential energy functions representing interparticle interactions at atomic scale should depend on local electric fields, but usually the approximation of fixed point charges and unpolarizable particles is adopted. This approximation appears to be too crude in several cases, and some ways to include at least linear polarization were explored.

At least three main routes to represent linear polarization have been proposed: (i) the shell model,[4] (ii) the self-consistent induction,[5] and (iii) the variable charge model.[6]

When the shell model is used in MD simulations, the positions of the (massless) shells must be optimized at each step or every few, so that the calculations become much longer than in the case of fixed point charges. In the self-consistent induction model[5] a self-consistent procedure is necessary in order to derive the correct values of the dipoles, resulting again in large computer time consumption.

In models where the values of the charges on particles are variable and are transferred from a particle to other, if the transferred charges depend on the distances between particles, the total potential energy can be expressed in terms of interparticle distances only. Therefore, the charge-transfer forces are conservative, and the usual MD procedures can be followed, provided that the evaluation of the Coulomb energy is suitably modified. Otherwise, if the charges depend on the electric field, like in Ref. 7 for water, self-consistency is not avoided.

Sprik and Klein[8] and Berne *et al.*[9] have proposed another model where polarizable atoms are made by positively charged nuclei surrounded by negative distributed charge sites with fixed positions relative to the atom but with values which are varied following a fictitious dynamics, so that the total instantaneous electric field is uniquely defined by the charges and self-consistency is avoided. A drawback of these models is to enlarge significantly the number of the degrees of freedom.

Here we propose a generalized model including linear polarization and other possible effects of the electric field on interparticle potential functions. If these effects do not modify directly the electric field itself, self-consistency is avoided; otherwise it can be included or overcome by using a Sprik–Klein scheme.[8]

The development of the present model started when we attempted to reproduce by MD simulations the structure and the internal vibrational spectrum of water molecules adsorbed in crystalline porous aluminosilicates (zeolites).

The chemical composition of zeolites[10,11] usually consists of silicon, aluminum, oxygen, and exchangeable cations. The crystalline framework is built up by corner sharing TO_4 tetrahedra (in which the *T*-sites are occupied by either silicon or aluminum), giving rise to a rather complex but

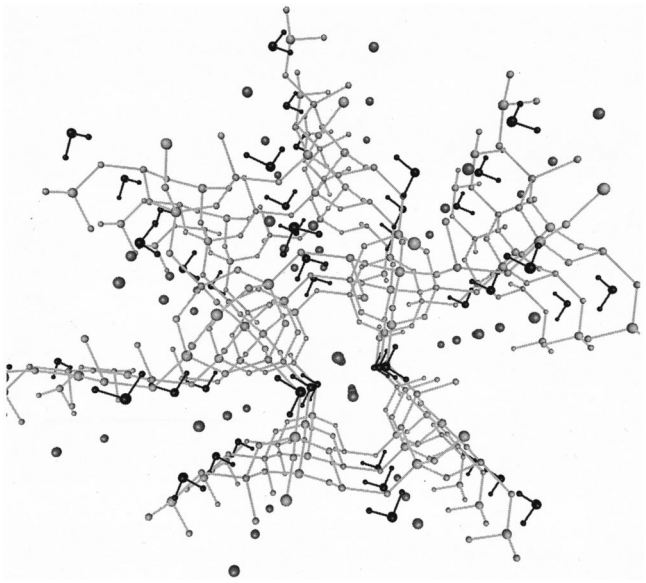

FIG. 1. The structure of natrolite as seen from the crystallographic axis *c*.

precisely repetitive atomic network with regular cavities joined by channels in which guest molecules of appropriate size can be accommodated. These void interior spaces can admit water, many gases, larger molecules, and cations (usually metallic) which compensate for the charge deficit due to the aluminum/silicon substitution. The MD simulations of zeolites have been extensively performed,[12] but not often for systems containing water.

However, the behavior of water in these materials is important, besides the mineralogical analysis, because the metallic cations present near the surface of the pores, when hydrated, can be removed and exchanged with other metallic or even more complex ions of great chemical interest. Moreover, water is involved as a local solvent or as a reactant in chemical reactions catalyzed by zeolites. Usually adsorbed water molecules are close to metallic cations generating a strong local electric field.

We attempted our first MD simulation of water in zeolites[13] in 1986 by selecting natrolite, a natural fibrous zeolite[10] whose structure[14] and properties[10] are known, and by testing some available point charge models for flexible water. The structure of natrolite is represented in Fig. 1. A simplified model was used, in which the crystalline framework, including the charge compensating Na^+ cations, was kept fixed (a quite common approximation), and water interacted only with the Na^+ cations, with charge $+e$, and with oxygen atoms of the framework, bearing a charge of $-0.2e$. It appeared that the point charge models for flexible water could not reproduce the experimental trend of the influence of electric fields on water molecules, which was confirmed by *ab initio* quantum mechanical calculations (see Ref. 15 for more details) to enlarge the HOH angle, to increase slightly the OH bond lengths, to red-shift the stretching vibrational frequencies, and to blue-shift slightly the bending mode frequency. Contrary to this trend, the HOH angle diminished, and the internal stretching vibration frequencies became higher.[13] Apparently, the inclusion of a nonlinear polarization effect modifying the electronic distribution of the molecule and affecting its structure and bond strength was necessary in order to explain the observed phenomena.

In order to apply these corrections to MD simulation, we derived a general dynamical model including potential energy terms depending on local electric fields,[15] which is illustrated in Sec. II. The scope of the investigation reported in this paper was to verify the actual application of the proposed model to MD simulation of large systems and to fit an intermolecular potential for liquid water to complement the electric-field-dependent intramolecular one derived in Ref. 15. Indeed, as better explained in Sec. II, among the potentials currently in use in the field none was found suitable without change for this purpose.

The use of flexible water models deserves some comments because it is subject to frequent criticism, especially when adopted for classical mechanics simulations. Indeed, the classical picture confines the vibrational motion to the bottom of the potential energy wells, neglecting the quantum zero-point energy, which is, for water, much higher than the average thermal energy. Therefore, the amplitude of the oscillations is not reproduced correctly, and a vibrational energy exchange with the surrounding particles is possible at any temperature, while, according to the quantum theory, the vibrational level differences are so high that at room temperature practically all molecules remain in the ground state and energy exchanges are rare events.

However, as long as the potential energy is close to a harmonic form, the vibrational frequency is substantially the same for classical and quantum theory, and the deformations of a potential energy function due to an electric field cause similar changes of the frequencies in both cases, so that if these changes are used as a probe of the electric field strength, one may compare them with the corresponding experiments.

Moreover, the potential functions proposed in this paper can also be adopted for quantum or semiclassical calculations. For instance, the vibrational level can be evaluated by numerical integration of the Schrödinger equation (an example for a molecule adsorbed in a zeolite is reported in Ref. 16), quantum corrections can be applied following the Feynman–Hibbs approach,[17] or approximated quantum calculations can be performed by the path integrals method.[18–21]

Finally, one can ask why are we discussing empirical potentials, when the first principles MD simulations (e.g., using the Car–Parrinello method) are feasible also for water.[22] The reasons are only in part practical. Indeed, actually Car–Parrinello calculations can handle systems containing at most about 100 atoms, but, even worse, the duration of the simulations hardly exceed a few picoseconds. However, even when thousands of atoms can be simulated for nanoseconds by first principles methods, empirical potentials will still be used to investigate the behavior of ''mesoscopic'' systems, containing millions of atoms for milliseconds, permitting us to explore an actually nearly unknown field, and to develop efficient theoretical and simulation methods to bridge the gap between the microscopic (atomic scale) and macroscopic worlds.

II. THE MODEL

Let us consider a system of N charged particles, interacting with each other via a potential energy function depending on their positions and on the electric fields acting upon each of them and generated by the other particles (which also depend on the positions of the particles):

$$V = V(\mathbf{r}_1,\ldots,\mathbf{r}_N|\mathbf{E}_1,\ldots,\mathbf{E}_N) = V(\{\mathbf{r}_i\}|\{\mathbf{E}_i(\{r_j\})\}) \quad (i,j=1,...,N), \tag{1}$$

where $\mathbf{r}_i$ are the positions of the particles and $\mathbf{E}_i$ are the electric fields. The force acting on a particle i is given by

$$\mathbf{f}_i = -\frac{\partial V}{\partial \mathbf{r}_i} = -\left(\frac{\partial V}{\partial \mathbf{r}_i}\right)_{\mathbf{E}} - \sum_j \frac{\partial V}{\partial \mathbf{E}_j}\frac{\partial \mathbf{E}_j}{\partial \mathbf{r}_i}, \tag{2}$$

where $\mathbf{E}$ stands for $\{\mathbf{E}_i\}$. In particular, it is worthy to note that the terms in Eq. (2) including the $3N\times 3N$ matrix,

$$\frac{\partial \mathbf{E}_i}{\partial \mathbf{r}_i},$$

corresponds to many-body forces involving in principle *all* the particles of the system as it is better illustrated if the atom pair approximation is assumed. In this approximation, the potential energy is represented by the sum of pairwise interactions $V_p(\mathbf{r}_{ij}|\mathbf{E})$ between particles i and j. Therefore, Eqs. (1) and (2) become

$$V = \sum_i \sum_{j>i} V_p(\mathbf{r}_{ij}|\mathbf{E}), \tag{3}$$

$$\mathbf{f}_i = -\left(\sum_{j>i}\frac{\partial V_p(r_{ij}|\mathbf{E})}{\partial \mathbf{r}_i}\right)_{\mathbf{E}} - \sum_{j>i}\frac{\partial V_p(\mathbf{r}_{ij}|\mathbf{E})}{\partial \mathbf{E}_i}\frac{\partial \mathbf{E}_i}{\partial \mathbf{r}_i} - \sum_{k\neq i}\sum_{j>k}\frac{\partial V_p(\mathbf{r}_{ki}|\mathbf{E})}{\partial \mathbf{E}_k}\frac{\partial \mathbf{E}_k}{\partial \mathbf{r}_i}, \tag{4}$$

where, again, $\mathbf{E}$ stands for $\{\mathbf{E}_i\}$ and the terms containing the electric field gradients have been grouped in two sums, the former including the gradient of the electric field acting on the particle i for which the force is calculated, and the latter including the gradients of the electric fields *acting on all the other particles multiplied by the derivatives, with respect to these electric fields, of the potential function terms involving the particle j, even though these terms do not include explicitly any interaction with the particle i*.

It is worthy to note that in general the last group of terms is not zero: indeed, it insures that the third law of the dynamics (as generalized for many-body forces) is obeyed.

As an example of application of the above-described model, we considered again the starting point which originated the development of the model itself, i.e., water adsorbed in aluminosilicates, which usually experiences strong electric fields.

In order to solve the problem of reproducing the structural and dynamical properties of the water molecule under the influence of an electric field, some potential terms depending on the electric field itself have been included[15] in a modified central force (CF) intramolecular model of water[23] (derived from the model by Stillinger and Rahman[24]). We stress that the model reported in Ref. 23 reproduces rather well (within about 4 kJ/mol) a sophisticated and accurate quantum mechanical potential energy surface for a wide range of configurations[25] of the water molecule and, therefore, the structure and the vibrational frequencies.

As mentioned above, the effect of the electric field is to enlarge the HOH angle, to increase slightly the OH bond lengths, to red-shift the stretching vibrational frequencies, and to blue-shift slightly the bending mode frequency. These phenomena are present, at least in part, in liquid water (possibly with the exception of the HOH angle, whose values, as derived from diffraction data, are reported in the 103°–105° range), but they are more evident for water adsorbed in zeolites.

Indeed, in some cases, water molecules are located in crystallographic positions and their structure can be accurately determined by neutron diffraction (see, for instance, Refs. 14 and 26). Usually, they are coordinated to the cations present on the internal surface of the micropores, and their distance from the cations, as well as the adsorption energy, are very similar to the corresponding ones for an isolated system containing one cation and one water molecule. This happens because of the high symmetry of the zeolite aluminosilicate frameworks, which makes the average electric field generated by the framework itself very small or negligible, so that the electric field acting upon an adsorbed water molecule is close to the one generated by the cations. This fact has been supported by experimental studies (see, for instance, Refs. 27 and 28) and has been exploited in performing *ab initio* calculations on Na^+–water systems in natrolite, a natural zeolite, neglecting the influence of the framework.[29]

Ab initio calculations for M^{n+}–water systems ($M^{n+}=Li^+, Be^{2+}, Na^+, Mg^{2+}$) including water flexibility and various configurations were performed by our group[15] and, previously, by Hermansson *et al.*[30] for ($M^{n+}=Li^+$, Be^{2+}, Mg^{2+}, Al^{3+}), confirming the experimental results (larger HOH angles, longer OH bond lengths) found in zeolites.

These calculations were used to find an *empirical* correction to describe the effect of an electric field on the intramolecular potential of a water molecule, avoiding self-consistent procedures like the one proposed by Robinson.[31] We assumed as a guideline the perturbation treatment used by Kahn, Cohen de Lara, and Möller[32] to interpret the IR spectra of small molecules adsorbed in zeolites. In particular, this treatment was followed to find a dependence of the HOH angle deformation on the electric field, which can be considered an indirect electronic effect. Indeed, it is caused by a complex interplay of electrostatic interactions involving (i) electronic density transfer from hydrogen to oxygen atoms; (ii) the corresponding increase of the positive net charge on the hydrogen atoms; (iii) a deviation from the sp^3 hybridization of the orbitals of the oxygen atoms, which in the isolated molecule is the main responsible for the HOH angle value; and (iv) the electrostatic forces acting on the nuclei.

Before reporting the derivation of the electric-field-dependent corrections, we must recall that the effect of the electric field on the charged H and O atoms (i.e., the Coulombic force, depending *linearly* on the electric field) is al-

TABLE I. Parameters for the *intramolecular* model potential of water [Eqs. (8) and (10), and (A1)–(A3) in the Appendix]. (Energies in kJ/mol when distances are in Å and electric field in units of $e/\text{Å}^2$.)

Parameter	1	2	3	Eq. (8)	Eq. (10)
a	151.144 90	302.289 80	132.124 28	365 213.37	2.568 52
b	28.2456	75.312	36.273 96	6.5×10^{-7}	28.2456
c	7.904 04	⋯	−376.56	446 534.21	7.904 04
d	34.033 66	⋯	0.9584	5.7×10^{-9}	
e	35.203 97	81.1986	10.0		
f	1.1	5.357 72	68.889 62		
g	11.938 42	1.452 51			
h	8.642 72	25.104			
m	2.2	1.5151			
n	1004.16	12.170 43			
p	0.9584				
q	29.558 29				

ways present; unfortunately, its acts so as to *reduce* the HOH angle, contrary to the actual experimental and theoretical trend.

Since the intramolecular potential functions contain the equilibrium HH distances for the isolated molecule (see the Appendix), these distances were increased by a quantity d_{HH}, whose dependence on the ''external'' electric field acting *upon the oxygen atom* was derived from the perturbation treatment by Kahn, Cohen de Lara, and Möller.[32] As ''external'' electric field we mean the field generated by the particles not belonging to a given molecule, or the total field acting on the oxygen atom from which the contributions of the hydrogen atoms of the same molecule are subtracted. Following the derivation of Ref. 32, we choose a set of internal coordinates of the water molecule to describe its deformation:

$$x_1=\Delta r_{\text{HH}},$$

$$x_2=\Delta r_{\text{OH}_1},$$

$$x_3=\Delta r_{\text{OH}_2},$$

where r_{HH} is the distance between the hydrogen atoms, and r_{OH_1} and r_{OH_2} are the distances between the oxygen atom and the hydrogen atoms.

The total intramolecular potential of a water molecule subjected to an electric field **E** as a function of the above-defined internal deformation coordinates may be represented as follows:

$$V_T=\frac{1}{2}\left\{\sum_{ij} K_{ij}+\left(\frac{\partial^2\mathbf{m}_0}{\partial x_i\partial x_j}\right)\cdot\mathbf{E}+\mathbf{E}^T\left(\frac{\partial^2\bar{\bar{\alpha}}_0}{\partial x_i\partial x_j}\right)\mathbf{E}\right\}x_ix_j+V_{\text{an}}, \tag{5}$$

where K_{ij} are the elastic constants in the minimum, $\mathbf{m}_0$ is the equilibrium dipole moment of the molecule, $\bar{\bar{\alpha}}_0$ is the polarizability tensor at equilibrium, and V_{an} is the anharmonic contribution to the potential energy.

The equilibrium dipole moment is a linear function of the chosen internal coordinates, so that

$$\left(\frac{\partial^2\mathbf{m}_0}{\partial x_i\partial x_j}\right)=\mathbf{0}.$$

Moreover, we suppose that the polarizability tensor is diagonal and is independent of $x_1=\Delta r_{\text{HH}}$ because the polarizability depends essentially on the electronic distribution around the oxygen atom.

In order to obtain the values of x_1,x_2,x_3 at equilibrium, the derivatives of Eq. (5) with respect to x_1,x_2,x_3 are set equal to zero, and by considering the above-mentioned approximations, it results in

$$\begin{aligned}
0&=K_{11}x_1+K_{12}x_2+K_{13}x_3+\frac{\partial V_{\text{an}}}{\partial x_1},\\
0&=K_{21}x_1+\left\{K_{22}+\left(\frac{\partial^2\bar{\bar{\alpha}}_0}{\partial x_2^2}\right)E^2\right\}x_2\\
&\quad+\left\{K_{23}+\left(\frac{\partial^2\bar{\bar{\alpha}}_0}{\partial x_2\partial x_3}\right)E^2\right\}x_3+\frac{\partial V_{\text{an}}}{\partial x_2},\\
0&=K_{31}x_1+\left\{K_{32}+\left(\frac{\partial^2\bar{\bar{\alpha}}_0}{\partial x_3\partial x_2}\right)E^2\right\}x_2\\
&\quad+\left\{K_{33}+\left(\frac{\partial^2\bar{\bar{\alpha}}_0}{\partial x_3^2}\right)E^2\right\}x_3+\frac{\partial V_{\text{an}}}{\partial x_3}.
\end{aligned} \tag{6}$$

By solving the system (6) with respect to x_1, one obtains the following dependence on the electric field modulus *E*:

$$x_1(E)=\frac{mE^4+nE^2+p}{qE^4+rE^2+s}, \tag{7}$$

where the symbols *m*,...,*s* are constants. The values of these constants were fitted to quantum mechanical calculations performed by our group for M^{n+}–water systems ($M^{n+}=\text{Li}^+,\text{Be}^{2+},\text{Na}^+,\text{Mg}^{2+}$) and to experimental data (see Ref. 15 for more details). It was found that the constant *p* became negligible, so that, after renaming $x_1(E)$ as $d_{\text{HH}}(E)$, the final result was

$$d_{\text{HH}}(E)=aE^2\frac{E^2+b}{cE^4+E^2+d}. \tag{8}$$

The terms of the potential function containing $d_{\text{HH}}(E)$ are described in the Appendix and the values of the parameters are reported in Table I. These modified terms insure the

correct values of the HOH angle and the correct trend of a slight increase of the bending frequency for increasing electric field.

In order to obtain the correct values of the stretching frequencies and of the OH bond length we could not use the same method, because the corresponding term (see the Appendix) does not include the equilibrium OH distance. Instead, it was found that a correcting additive term of the form

$$V_{\mathrm{OH}}(E) = -a\frac{bE^2}{r^c} \tag{9}$$

corresponding to a decrease of the intramolecular repulsive term

$$V_{\mathrm{OHrep}} = \frac{b}{r^c} \tag{10}$$

yielded both a control of the elongation of the bond induced by the electric field and a lowering of the stretching frequencies caused by the negative curvature of the added term. The values of the parameters which enter in Eqs. (8) and (10) are reported in Table I, and were derived, as reported in Ref. 15, by fitting *ab initio* calculations and some spectroscopic data for water adsorbed in zeolites.

The electric-field-dependent terms are essentially intramolecular and short ranged; however, an indirect effect on intermolecular interactions is caused by the changes of the structure of each molecule and by the *N*-body forces arising from the last term of Eq. (4).

Once an electric-field-dependent intramolecular model for water was available, intermolecular interactions had to be added. Among the models proposed in literature, the one by Wallqvist and Berne[33] (WB), developed in two forms, with and without polarization, was chosen. It is very simple: the centers of force correspond to the atoms, and the reproduction of the properties of liquid water is good, both for the form including polarization and for the fixed charge version. For the sake of simplicity, we preferred to avoid including linear polarization and to consider a fixed charge model.

Unfortunately, the values of the charges used in the WB potential are very different from those adopted by the CF model for the intramolecular terms ($q_{\mathrm{O}} = -0.92e$ and $q_{\mathrm{OH}} = -0.65966e$, respectively). This difference stems from reproduction of the dipole moment of the water molecule in the liquid, which corresponds to the WB charges, and of the isolated molecule, corresponding to the CF model charges. We preferred to maintain the CF choice at least for two reasons: (i) the high value of the dipole moment in the liquid is due to polarization effects, which vanish at a distance rate faster than the point charge potentials; and (ii) at large distances the CF charges are preferable, as recently pointed out by Guillot and Guissani, mainly because they give a better description of the high-temperature low-density phase.[17] Therefore, while assuming the form of the WB model but maintaining the CF charges values, we were obliged, unwillingly, to fit again the parameters of the WB potential and to add some terms in order to obtain a reasonable intermolecular potential for liquid water. The final form of the water–water intermolecular potential is the following:

TABLE II. Parameters for the *intermolecular* model potential of water [Eqs. (11)–(13)]. (Energies in kJ/mol when distances are in Å.)

Parameters	A	B	C	D	E	F
V_{OO}	3 500 000	3100	15.0	2.093	1.5	4.5
V_{OH}	19 098.33	4.06	223.796			
V_{HH}	2 134.86	2.76	4.186	1.5	3.15	
Charges		q_{O}			q_{H}	
(units of e)		−0.65966			0.32983	

$$V_{\mathrm{OO}}(r) = \frac{q_{\mathrm{O}}q_{\mathrm{O}}}{4\pi\varepsilon_0 r} + \frac{A}{r^{12}} - \frac{B}{r^6} + \frac{C}{r^4} - D\exp[-E(r-F)^2], \tag{11}$$

$$V_{\mathrm{OH}}(r) = \frac{q_{\mathrm{O}}q_{\mathrm{H}}}{4\pi\varepsilon_0 r} + A\exp(-Br) - \frac{C}{r^4}, \tag{12}$$

$$V_{\mathrm{HH}}(r) = \frac{q_{\mathrm{H}}q_{\mathrm{H}}}{4\pi\varepsilon_0 r} + A\exp(-Br) + C\exp[-D(r-E)^2]. \tag{13}$$

The values of the parameters are reported in Table II. We may note that the Gaussian function in the O–O interaction, which was present in the original WB model, is centered, as in the original one, at $F = 4.5$ Å, a value corresponding to the O_1-O_3 distance between two oxygen atoms, O_1 and O_3, both linked by hydrogen bonds to a third oxygen O_2. This little dip in the potential energy (the parameter D is only about 2 kJ/mol) controls the variations of $O_1-O_2-O_3$ angle which, as stated by Robinson *et al.*,[34] should be one of the keys to understanding the behavior of liquid water, and, by some elementary geometrical considerations, it can be shown that this minimum is roughly equivalent to the minimum at 3.4 Å in the O–O potential function proposed in Ref. 34 just to monitor O–O–O angles. Indeed, this distance corresponds to the shorter diagonal of the parallelogram with sides O_1-O_2 and O_2-O_3.

As in all the recent studies in this field, the fitting was carried out directly for liquid water, and in our case for one more reason: the unknown effect of the many-body forces arising from the last term of Eq. (4). The fitted properties were cohesive energy, radial distribution functions, and diffusion coefficients. Internal pressure and HOH angle were also monitored. Once the potential parameters were derived, we verified its ability to reproduce the properties of the water dimer, as shown in Sec. IV A.

A potential model including electric point charges for the aluminosilicate framework had been derived by some of the authors[35] by fitting structural and vibrational properties of silicalite, zeolite, Na A, and Ca A, obtaining satisfactory results. Therefore, in order to simulate hydrated zeolites, besides a model for water, it was necessary to add water–cation and water–framework potentials. *Ab initio* and experimental data (both structural and vibrational) were easily fitted, using the following form, for representing the interactions between an ion and the oxygen and hydrogen atom of a water molecule:

TABLE III. Parameters for Na^+–water interactions [Eq. (14)]. (Energies are in kJ/mol when distances are in Å.) The charge of Na^+ is $+e$.

Parameters	A	B	C
Na^+–O	489 528.0	4.526	−376.56
Na^+–H	416 987.5	7.07	292.88

$$V_{Na^+O,H}(r)=\frac{q_{Na^+}q_{O,H}}{4\pi\varepsilon_0 r}+A\exp(-br)-\frac{C}{r^4}. \tag{14}$$

The values of the parameters for the Na^+–water interaction are reported in Table III. In Table IV the structural and vibrational properties of the Na^+–water system obtained using the above-described model are illustrated. They reproduce satisfactorily experimental and *ab initio* results. The parametrization actually includes also Li and Ca ions and will be extended to other ions, but we prefer to delay their publication after extensive tests on zeolites will be available.

Finally, the water–framework potentials were fitted to structural and vibrational data of natrolite[14] and scolecite.[26] We choose these zeolites because their structure (with ordered positions for Al and Si atoms) was studied at low temperatures by neutron diffraction, allowing an accurate determination of atomic positions (and in particular of the positions of hydrogen atoms), since water molecules at room and lower temperature are in ordered crystallographic positions. Moreover, experimental vibrational spectra are available. The aluminosilicate structures of both zeolites is the same, but natrolite contains sodium cations whereas scolecite contains calcium cations.

Water was assumed to interact with Si and Al atoms via a Coulomb potential only (the values of the charges are reported in Table V), and the potential functions between the oxygen atoms of the framework and the oxygen or hydrogen atoms of water were derived from a simplified form of the corresponding O–O and O–H ones for water–water interactions.

TABLE V. Parameters for the interactions between an oxygen atom of the zeolitic framework (O_f) and an oxygen atom (O) or a hydrogen atom (H) of water [Eqs. (15) and (16)]. (Energies are in kJ/mol when distances are in Å.)

Parameters	A	B	C
O_f–O	3 500 000	3100	15.0
O_f–H	984.9	179.9	⋯
Charges	q_{O_f}	q_{Si}	q_{Al}
(units of e)	−1.0	1.8	1.3

The potentials for interactions between an oxygen atom of the zeolite framework (O_f) and an oxygen (O) or a hydrogen (H) atom of the water molecule were represented by

$$V_{O_fO}=\frac{1}{4\pi\varepsilon_0}\frac{q_O q_{O_w}}{r}+\frac{A}{r^{12}}-\frac{B}{r^6}+\frac{C}{r^4}, \tag{15}$$

$$V_{O_fH}=\frac{1}{4\pi\varepsilon_0}\frac{q_O q_{H_w}}{r}+\frac{A}{r^7}-\frac{B}{r^4}, \tag{16}$$

and the values of the parameters are reported in Table VI. Both the form of the potential functions and the values of the parameters are to be considered as preliminary and subject to further adjustments, because we performed only test calculations, except for natrolite.

In conclusion, the total potential energy of a hydrated aluminosilicate is given by

$$V=V_f+V_{OO}+V_{OH}+V_{HH}+V_{IO}+V_{IH}+V_{FO}+V_{FH}+V_{OH}^{intra}(E)+V_{HH}^{intra}(E)+V_{HOH}^{intra}, \tag{17}$$

TABLE IV. Results for Na^+–water system *in vacuo*. (* denotes assumed and fixed values.)

	Na^+–O (Å)	O–H_1 (Å)	HOH (degrees)	E (KJ/mol)	Water molecule frequencies (cm^{-1})			
					ν_1	ν_2	ν_3	NA^+–Water
Experiment	2.28[a]	≈0.99[b]	≈108[b]	−24.0[a]	≈1630[c]	≈3300−3500[c]		305±15[d]
				−23.4[e]				
ab initio[f]	2.21	0.947	106.6	−28.6	⋯	⋯	⋯	
ab initio[g]	2.23	0.96*	104.5*	−25.8	⋯	⋯	⋯	
ab initio[h]	2.23	0.96*	104.5*	−25.1	⋯	⋯	⋯	
ab initio[i]	2.21	0.96*	104.5*	−28.7	⋯	⋯	⋯	
ab initio[j]	⋯	0.96*	104.5*	−24.7	⋯	⋯	⋯	
DFT[k]	⋯	0.96*	104.5*	−24.4	⋯	⋯	⋯	
DFT[l]	2.25	0.96*	104.5*	−23.4	⋯	⋯	⋯	
This work	2.21	0.987	107.1	−24.2	1673	3420	3460	320

[a]Reference 58.
[b]Reference 14 for water adsorbed in natrolite and coordinated to Na^+ cation.
[c]Reference 10 for water adsorbed in natrolite and coordinated to Na^+ cation (see text).
[d]Reference 59.
[e]Reference 60.
[f]Reference 13.
[g]Reference 61.
[h]Reference 62.
[i]Reference 63.
[j]Reference 64.
[k]Reference 65.
[l]Reference 66.

TABLE VI. Results for liquid water ($T=300$ K). (* denotes assumed and fixed values.)

	Density (g/cm^3)	r_{OH} (Å)	$\theta_{H\hat{O}H}$ (degrees)	ΔE_{sol} (kJ/mol)	D (10^{-9} m^2/s)
Experiment	0.997[a]	0.966[a]	102.8[a]	41.5[c]	2.4[d]
		0.98[b]	105.5[b]		
This work	0.997*	0.98	102.9	42.6	2.24
CF	1.000*	0.96[e]	99.9[f]	39.7[e]	1.12[e]
WB(pair)[g]	1.000*	0.96*	104.52*	41.6	2.4
WB(pol)[g]	1.000*	0.96*	104.52*	41.2	2.8
MCYL[h]	0.998*	0.975	103.5	22.73	1.9
TIP4P[c]	0.997	0.96*	104.52*	41.6	3.3 ± 0.5
SPC/E[i]	0.997	1.0*	109.47*	46.7	2.4

[a]Reference 41.
[b]Reference 42.
[c]Reference 67.
[d]Reference 43.
[e]Reference 24.
[f]Reference 68.
[g]Reference 33; WB(pair) is the fixed charge potential, WB(pol) is the version including polarization.
[h]Reference 69.
[i]Reference 40.

where V_f is the overall potential energy for the aluminosilicate framework (see Ref. 35), V_{OO}, V_{OH}, and V_{HH} are sum of the pairwise potentials defined by Eqs. (11)–(13), V_{IO} and V_{IH} are the same ones corresponding to Eq. (14), and V_{FO} and V_{FH} indicate the contribution of the interactions between water and the atoms of the framework [Eqs. (15) and (16) for oxygen atoms, Coulombic only for Si and Al]. The last three terms, which depend on electric fields, stem from the Eqs. (A1)–(A3) of the Appendix.

For condensed state simulations, the evaluation of the electric fields and their gradients was performed by using Ewald summations including all charges and then subtracting the intramolecular contributions. The **k**-space terms of the electric field gradients are computationally demanding, and special methods are required in order to speed up the calculations. In particular, it turned out that the convergence of the **k**-space sums for the electric field gradient was ensured by a lower value of $|\mathbf{k}|$ as compared with the corresponding one for the electric field evaluation. Moreover, the contribution of **k**-space sums to the electric field gradient changes relatively slowly, and the total energy conservation is good even if it is not updated each step, but about every ten steps.

When the calculations reported in this paper were finished, an interesting paper proposing a new method for evaluating Coulombic potentials was published.[36] This method is very appealing for its simple form and appears suitable especially for liquids, and for water in particular, as it should yield better results when the minimum distance between opposite charges is smaller. Test calculations show that it could shorten the computing time by about three times for liquid water, obtaining practically the same results as using the Ewald method. A detailed study of the application of this method is in progress.

III. CALCULATIONS

Standard MD simulations were performed for three kinds of systems: liquid water, isolated water dimer, and hydrated natrolite. A modified Verlet algorithm in velocity form[37] with time step of 0.5 fs was used and, for liquid water, NVE ensemble with periodic boundary conditions, minimum image convention, and Ewald summation for the evaluation of electric potential energy, electric field, and field gradient were adopted.

For bulk water, a cubic MD cell with side equal to 21.752 Å, containing 343 molecules, corresponding to a density of 0.997 g cm^{-3}, was chosen. For bulk water, after about 14 ps of equilibration, a production run of 48 ps at room temperature (300 K) was performed. The computer time required by one step was, for bulk water, about 2.5 s on a DS20 COMPAQ workstation. The energy conservation error was less than 0.01%.

The IR spectrum was computed as Fourier transform of the total dipole autocorrelation functions, the diffusion coefficient of bulk water was evaluated with the usual Einstein formula, and the internal pressure was derived from the virial theorem (see Refs. 3, 12, and 38 for the details of the treatment of MD simulations data).

In order to find the optimized frozen structure of a water dimer a simulated annealing procedure was adopted.[39] After minimization, the vibrational frequencies were evaluated by simulation runs 5 ps long, starting from configurations chosen in order to excite only one vibrational mode for each run, at a temperature corresponding to the room temperature.

The MD simulations of natrolite were performed at different temperatures, namely 166 K, 307 K, and 650 K, in order to compare the results of the calculation with the available experimental data (the diffraction data for the structure determination were collected at 20 K and at room temperature, and the vibrational spectra were recorded at room temperature), and to check the mobility of water at high temperature. Indeed, it is well known[10] that at about 600 K at least some water has evaporated from the zeolite. The simulation at 166 K was compared with the experimental structure at 20 K, taking into account the quantum zero point vibrations of the real crystal which cannot be reproduced by classical MD calculations. The equivalence of the two tem-

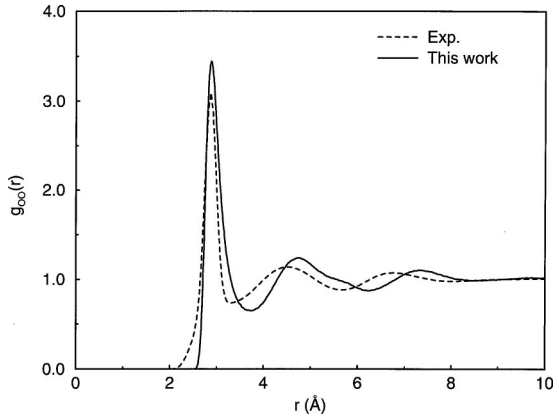

FIG. 2. Oxygen–oxygen radial distribution function of liquid water, present work results (continuous line) compared with an experimental data set (Ref. 44) (dashed line).

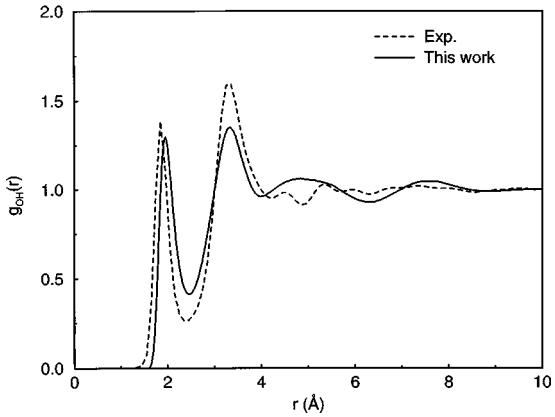

FIG. 3. Oxygen–hydrogen radial distribution function of liquid water, present work results (continuous line) compared with an experimental data set (Ref. 44) (dashed line).

peratures was estimated by comparing experimental and computed vibration mean square amplitudes.

Natrolite structure belongs to the monoclinic symmetry group Fdd2, but the β angle is just 90°. The cell dimensions are $a=18.26$ Å, $b=18.64$ Å, and $c=6.59$ Å, respectively, and the cell contains 16 Na ions, 16 Al atoms, 32 Si atoms, 80 O atoms, and 16 water molecules (in total 136 atoms). The MD box corresponded to three crystallographic cells superimposed along the *c* axis in order to obtain an approximately cubic one of $18.26\times18.64\times19.77$ Å, including 552 atoms. The time step was 0.5 fs, and the simulations were 20 ps long, after 5 ps for equilibration, but the simulation at 307 K was prolonged up to 400 ps in order to check the dependence of the computed quantities on the duration of the run. Neither the structural properties nor the spectrum did change significantly by increasing the simulation length.

IV. RESULTS AND DISCUSSION

A. Liquid water

As mentioned above, our main interest was in the simulation of water molecules adsorbed in aluminosilicates, where usually the water–water interactions are not critical for a good reproduction of the experimental data, but, in order to test more extensively the model proposed in this work, a simulation of liquid water at room temperature was performed.

The results are reported in Table VI, and are compared with those obtained by some other models, including the most relevant flexible water potentials not considering polarization, the WB potentials, and two of the most popular rigid water potentials, and in Figs. 2–5. The cohesive energy of bulk water was computed as the difference between the energy of a gas of 343 water molecules at room temperature and the total energy of the simulated liquid water, in order to take into account the deformation energy of the molecules due to the interactions with other molecules including the electric field effects. As it appears in Table VI, it is slightly lower than the experimental one (by about 1 kJ/mol), but it falls within the error bounds of the results of most recent simulations.[40] The deformation of the water molecule is in line with the experimental evidence of a slight stretching of the OH bond. As for the HOH angle, the treatment of the experimental data yields different values, ranging from 102.8°[41] to 105.5°[42] and the computed value approaches (and actually was fitted to) the lower value. The computed diffusion coefficient, $D=2.24\times10^{-9}$ m^{2}s^{-1}, is close to the experimental value of $D=2.4\times10^{-9}$ m^{2}s^{-1}.[43]

The radial distribution functions are shown in Figs. 2–4 and are reasonably similar to the experimental ones,[44] and in line with the results of other MD simulations performed with empirical potentials.

In Fig. 5 the simulated and experimental IR spectra[45–49] in different frequency ranges are reported, and the results appear to be satisfactory. In particular, the O–H stretching band, in the frequency range 3400–3700 cm^{-1}, is red-shifted with respect to the gas phase frequencies (3660 and 3754 cm^{-1}) reported in Ref. 23.

In summary, the results of the simulations reported in this work are in line with those of the most used models, as discussed, for instance, in a recent paper[40] where the performances of different potentials are compared. It appears that for some of them there is at least one computed value that is

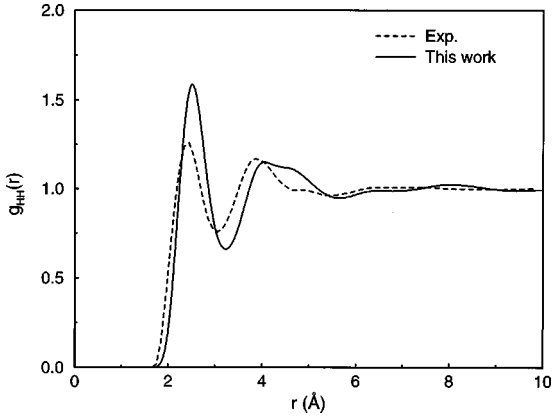

FIG. 4. Hydrogen–hydrogen radial distribution function of liquid water, present work results (continuous line) compared with an experimental data set (Ref. 44) (dashed line).

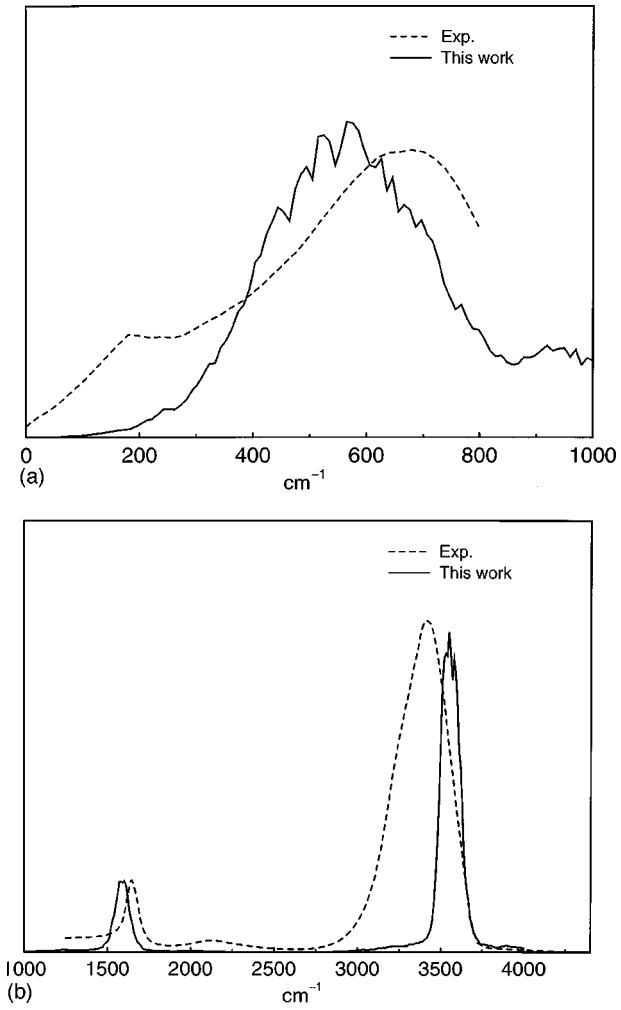

FIG. 5. Computed infrared spectrum of liquid water, in arbitrary units (continuous line), in different frequency ranges compared with averaged experimental data (Refs. 45–49). (a) 0–1000 cm^{-1}; (b) 1000–4400 cm^{-1}.

poorly reproduced. For the present model the weak point is the computed pressure, which is too high (about 600 MPa).

As pointed out by Robinson *et al.*,[34] ''the'' model for liquid water is still lacking, because not only water shows *per se* a very complex behavior, but also the results for a given model may depend strongly on the simulation method.

For instance, in Ref. 17, quantum corrections proposed by Sesé[50] yield, for a given potential, a softening of the radial distribution functions especially in the first hydration shell, an increase of the diffusivity (by nearly 100% at room temperature), and a decrease of the heat of vaporization (by nearly 10% at room temperature). The same trend is observed if quantum effects are simulated by the path integral method.[20,21]

Therefore, in our opinion, the proposed models should be adjusted at best in order to fit the experimental values of interest in a series of computer experiments once a simulation method is chosen, waiting to improve the method itself. For water, a ''good'' MD simulation method should take in account, at the same time (i) the quantum nature of the intramolecular vibrations (both for the oscillation amplitude and zero point energy),[51] (ii) the quantum behavior of hydrogen atoms;[17,20,21] (iii) the polarization and the oscillations of the charge distributions,[7–9] and possibly other effects: all these requirements would make any simulation a formidable task, using the actually available computers. Beyond analytical representation of the potential energies (and possibly as a basis to refine them) path integral Car–Parrinello molecular dynamics simulations[52,53] could be the good technique, if it were not so computer resources demanding.

TABLE VII. Results of water dimer: Structural data and binging energy for water dimer.

	O_1–O_2 (Å)	θ_c[a] (degrees)	θ_d[a] (degrees)	γ[a] (degrees)	ΔE (kJ/mol)
Experiment	2.98[b,c]	57±10[b] 58.5±6[c]	51±10[b] 50.2±6[c]	6±10[c]	−23±3[d]
This work	2.93	27.3	53.1	0.9	−17.25
CF[e]	2.84	30.9	48.1	−3.6	−23.57
WB(pair)[f]	2.80	21	48	0	−30.9
WB(pol)[f]	2.95	19	47	0	−14.7
MCYL[g]	2.87	37	56.0	4	−24.85
TIP4P[h]	2.75	46	52.2	0	−26.1
SPC/E[i]	2.75	22	52.2	0	−30.0

[a] θ_c and θ_d are the angles between the O–O distance and the bisector of the acceptor and donor molecule, respectively; γ is the angle between O–O and O–H_3 distances, where H_3 is the hydrogen atom involved in the hydrogen bond.
[b] Reference 54.
[c] Reference 55.
[d] Reference 70.
[e] Computed using the modified central force (CF) proposed in Ref. 24.
[f] Reference 33; WB(pair) is the fixed charge potential, WB(pol) is the version including polarization.
[g] Reference 69.
[h] Reference 67.
[i] Reference 71.

B. Water dimer

The results for the water dimer are summarized in Tables VII and VIII, and are compared with those of the original modified CF model by Stillinger and Rahman,[24] with those of some other models including the WB potential, from which the present one was derived, and with experimental data. As usual for potentials designed for condensed state simulations, the computed O–O distance (2.93 Å) is shorter than the experimental one (2.98 Å),[54,55] but unexpectedly better than for other models[56] (by recalling that it was *not* a fitted value, and in the liquid the first maximum of the O–O radial distribution function is 2.85 Å). The other structural parameters are in line with other potentials fitted to the properties of liquid water. The energy of cohesion is lower than the experimental one, probably because in the liquid the many-body electric-field-dependent forces are slightly overestimated.

On the other hand, the computed vibrational frequencies (see Table VIII), though they were *not* fitted during the parameter optimization, are much closer to the experiment than those derived from other models.[56]

C. Water in natrolite

In order to check the validity of the above-described model when applied to water adsorbed in zeolites, we per-

TABLE VIII. Results of water dimer: vibrational frequencies (cm^{-1}).[a]

	ν_{12}	ν_{11}	ν_{10}	ν_9	ν_8	ν_7	ν_6	ν_5	ν_4	ν_3	ν_2	ν_1
Calculated[a]	86	480	170	280	324	434	1530	1500	3572	3570	3680	3657
CF[c]	87	281	120	307	327	509	1409	1483	4332	4303	3853	3856
Experiment	n.a.	n.a.	150	n.a.	290	520	1593	1611	3545	3600	3730	3714
			147		320		1601	1619	3532	3600	3722	3730
			155						3574	3634	3726	3709
									3556	3627	3715	3699

[a]Experimental values and the numbering of normal modes are taken from Ref. 56 and references therein.
[b]This work.
[c]Computed using the modified central force (CF) proposed in Ref. 24.

formed, as reported earlier, some preliminary calculations on several zeolites, including scolecite and natrolite, but only for the last one the simulations were achieved and analyzed in details.

The simulated structure of natrolite results are remarkably stable, like the experiment, showing thermal factors increasing with temperature, and with the correct order of magnitude. The symmetry of the crystal, which is not imposed, is conserved accurately. Average coordinates are close to the experimental ones, and distances and angles differ from experiment at most by some 0.01 Å and a few degrees, respectively. As in this paper the interest is focused on the behavior of water; we shall not discuss the results related to the aluminosilicate framework any further.

The diffusion of water was not observed even at 650 K, probably because the simulations were not sufficiently long (they lasted about 20 ps), but the distribution functions of the coordinates of oxygen atoms of water at that temperature are large and those of hydrogen atoms are flat, suggesting librations of very large amplitude or free rotation.

The structural and vibrational properties of water obtained by the new model are compared with the experimental data and with the results of the previous simulations[13] in Table IX and in Fig. 6. As it appears in Table IX, the experimental O–H distances corrected for thermal vibrations of the only crystallographically independent water molecule are very well reproduced, within some 0.003 Å, and with the correct length order. Moreover, HOH angles are larger than in the isolated water molecule and in liquid water and are close to the experimental results. Especially for angles, the present results are better than the previous ones.

The computed (IR) spectrum is reported in Fig. 6 along with the experimental one and that obtained in the previous work (Ref. 13). The one obtained in the present study is rather good, although with some frequency shifts with respect to experiment and with some intensities sometimes too high or too low. The improvement over the previously computed spectrum is dramatic, especially for the stretching band at 3300–3600 cm^{-1}. However, for the last one, whereas the newly computed band is centered at the right frequency, it is too narrow and not sufficiently structured when compared with the experimental one.

We attribute this discrepancy, and the slight blue-shift of the bending band at about 1650 cm^{-1}, to a possibly too stiff interaction between water and framework.

By comparing the results for the Na^+–water system *in vacuo* (Table IV) and for water in natrolite (Table IX) it appears that the effect of the aluminosilicate is nearly negligible: the structure and the vibrational frequencies of water are nearly the same. This finding is in line with previous experimental[27,28] and theoretical work, both for natrolite in

TABLE IX. Structural results for water in natrolite: bond lengths and angles for the adsorbed water molecule. Distances are in Å and angles in degrees.

	Room temperature			Low temperature	
	Experiment[a]	Calculated[b]	Calculated (this work)	Experiment[c]	Calculated (this work)
Distances					
OH_1	0.98±0.02	0.992[d]	0.993	0.995	0.992
OH_2	0.98±0.02	0.992[d]	0.990	0.991	0.989
Angles					
HOH	108	98.8	105.3	107.9	105.8

[a]Reference 72.
[b]Reference 13. Average of the results of six runs, lasting 35 ps in total.
[c]Reference 14.
[d]Average of the values of the two crystallography independent OH distances.

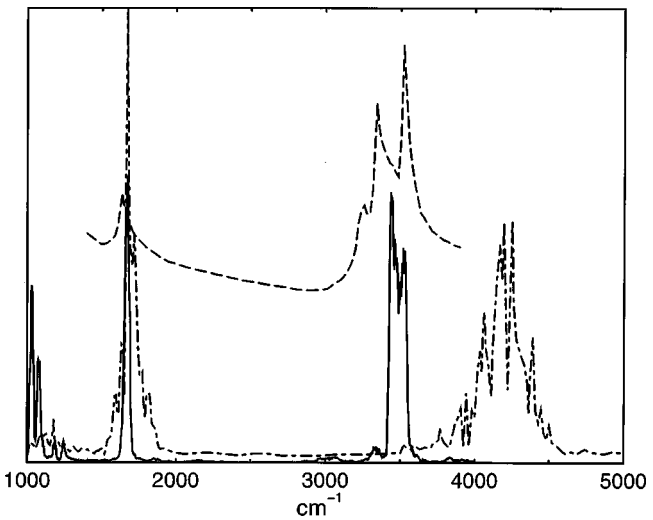

FIG. 6. Computed infrared spectrum of hydrated natrolite, in arbitrary units (continuous line), compared with experimental data (Ref. 10) (dashed line) and with previous results (Ref. 11) (dotted–dashed line) in the range 1000–5000 cm^{-1}.

particular[29] and for the extended use of relatively small clusters for representing specific sites of zeolites in *ab initio* calculations, which compare fairly well the full-crystal ones, when available.[57]

Work is in progress to refine the potential functions in order to attain a better reproduction of the experimental data and to extend the calculations to zeolites containing different ions or of different structural groups.

V. CONCLUSIONS

We stress that the present scheme [Eqs. (1)–(4)], which is able to yield satisfactory results in a special case, is of general form and could be useful for representing complex electric-field-dependent phenomena such as reactive potential energy surfaces, both empirical and quantum mechanical.

In particular, the results reported in the present paper show that the introduction of electric-field-dependent terms in the intramolecular potential of water can improve the reproduction of complex electronic effects by relatively simple empirical functions. The presence of *N*-body terms in the intermolecular terms forces resulting from the electric field gradient entails a modification of the intermolecular potentials for water, which, however, can be handled by adjusting empirical functions taken from literature, and yielding results similar to the best ones obtained from classical MD simulations.

As remarked above, the model can be improved by including polarization, but the results of the simulations, and in particular for water and other molecules containing hydrogen, may change depending on the simulation techniques. The presence of hydrogen entails both the quantum behavior of the hydrogen atoms (connected among the others with tunneling effects) and high vibrational frequencies (which imply high zero point energies and scarce energy exchange with the environment), so that a quantum or at least a semiclassical treatment should be demanded to reasonably simulate these kinds of molecules. These considerations, together with the approximations involved in atom pair and (besides Coulomb interactions) essentially nearest neighbor potential functions would explain, at least in part, why a fully satisfactory reproduction of the behavior of water is still lacking. On the other hand, quantum or semiclassical treatments are likely to be too demanding for the actual computer capabilities, and for (some) years empirical functions, possibly improved with a dependence on electric fields, when necessary, can be fruitfully used.

The preliminary results reported in this paper for the hydrated zeolite natrolite show that the problem that originated the present study, i.e., reproducing the behavior of confined molecules subject to an electric field by MD simulations using empirical potential functions, can be successfully approached. Taking into account the previously discussed approximations and limits, we will attempt to use the model reported in the present work for studying water adsorbed on the surface or in the pores of ionic and partially ionic solids, many of which, like metal oxides and aluminosilicates (clays, zeolites), are of high chemical interest.

ACKNOWLEDGMENTS

This research is supported by Ministero dell'Università e della Ricerca Scientifica e Tecnologica (MURST), by Università degli studi di Sassari and by Consiglio Nazionale delle Ricerche.

APPENDIX: POTENTIAL FUNCTIONS FOR THE INTRAMOLECULAR POTENTIAL OF WATER

The intramolecular potential model for water is rather complex. Though it may appear awful, in practice it can be fitted with splines, with the exception of the electric-field-dependent terms. The constant term b_2 is reminiscent of an intermolecular term of the original CF model,[24] and is necessary in order to give the correct dissociation energy of the molecule. The form of the potential is the following:

$$V_{\mathrm{OH}}^{\mathrm{intra}}(r|E) = -\frac{a_1}{r} + \frac{b_1}{r^{c_1}} - \frac{d_1}{\{1+\exp[-e_1(r-f_1)]\}} - \frac{g_1}{\{1+\exp[-h_1(r-m_1)]\}} + n_1(r-p_1)^2 \exp[-q_1(r-p_1)^2] + V_{\mathrm{OH}}(E), \tag{A1}$$

$$V_{\mathrm{HH}}^{\mathrm{intra}}(r|E) = \frac{a_2}{r} + b_2 - e_2 \exp\{-f_2[r-g_2-d_{\mathrm{HH}}(E)]^2\} + h_2[r-m_2-d_{\mathrm{HH}}(E)]^2 \times \exp\{-n_2[r-m_2-d_{\mathrm{HH}}(E)]^2\}, \tag{A2}$$

$$V_{\mathrm{HOH}}^{\mathrm{intra}}(r) = a_3 \exp[-b_3(r_{\mathrm{HH}}-r_{\mathrm{OH}_1}-r_{\mathrm{OH}_2})^2] + c_3[(r_{\mathrm{OH}_1}-d_3)+(r_{\mathrm{OH}_2}-d_3)]^2 \times \exp\{-e_3[(r_{\mathrm{OH}_1}-d_3)+(r_{\mathrm{OH}_2}-d_3)]^2\}. \tag{A3}$$

The values of the parameters are reported in Table I. The terms $d_{\mathrm{HH}}(E)$ and $V_{\mathrm{OH}}(E)$ are defined in Eqs. (8) and (10), respectively.

[1] B. J. Alder and T. E. J. Wainwright, Chem. Phys. **27**, 1208 (1957).
[2] M. P. Allen and D. J. Tildesley, *Computer Simulation of Liquids* (Clarendon, Oxford, 1987).
[3] *Computer Simulation in Chemical Physics*, edited by M. P. Allen and D. J. Tildesley (Kluwer, Dordrecht, 1994).
[4] B. G. Dick and A. W. Overhauser, Phys. Rev. **112**, 91 (1958).
[5] F. H. Stillinger and C. W. David, J. Chem. Phys. **69**, 1473 (1968).
[6] A. Alavi, L. J. Alvarez, S. R. Elliott, and I. R. McDonald, Philos. Mag. B **65**, 489 (1992).
[7] I. M. Svishchev, P. G. Kusalick, J. Wang, and R. J. Boyd, J. Chem. Phys. **105**, 4742 (1996).
[8] M. Sprik and M. L. Klein, J. Chem. Phys. **89**, 7556 (1988).
[9] S. W. Rick, S. J. Stuart, and B. J. Berne, J. Chem. Phys. **101**, 6141 (1994).
[10] G. Gottardi and E. Galli, *Natural Zeolites* (Springer-Verlag, Berlin, 1985).
[11] D. W. Breck, *Zeolites Molecular Sieves* (Wiley, New York, 1973).
[12] P. Demontis and G. B. Suffritti, Chem. Rev. **97**, 2845 (1997).
[13] P. Demontis, G. B. Suffritti, A. Alberti, S. Quartieri, E. S. Fois, and A. Gamba, Gazz. Chim. Ital. **116**, 459 (1986).
[14] Å. Kvick, K. Stahl, and J. V. Smith, Z. Kristallorg. **171**, 41 (1985).
[15] P. Demontis, G. B. Suffritti, E. S. Fois, A. Gamba, and G. Morosi, Mater. Chem. Phys. **29**, 357 (1991).
[16] A. V. Larin, F. Jousse, and E. Cohen De Lara, in *Zeolites and Related Microporous Materials: State of the Art 1994*, edited by J. Weitkamp, H.

G. Karge, H. Pfeifer, and W. Hölderlich (Elsevier, Amsterdam, 1994), p. 2147.
[17] B. Guillot and Y. Guissani, J. Chem. Phys. **108**, 10162 (1998).
[18] J. A. Barker, J. Chem. Phys. **70**, 2914 (1979).
[19] M. J. Gillan, Phys. Rev. Lett. **58**, 563 (1987).
[20] R. A. Kuharski and P. J. Rossky, J. Chem. Phys. **82**, 5164 (1985).
[21] S. R. Billeter, P. M. King, and W. F. Van Gunsteren, J. Chem. Phys. **100**, 6692 (1994).
[22] M. Sprik, J. Hutter, and M. Parrinello, J. Chem. Phys. **105**, 1142 (1996).
[23] P. Demontis, G. B. Suffritti, E. S. Fois, and A. Gamba, Chem. Phys. Lett. **127**, 456 (1986).
[24] F. H. Stillinger and A. Rahman, J. Chem. Phys. **68**, 666 (1978).
[25] W. P. Kramer, B. O. Roos, and P. E. M. Siegbahn, Chem. Phys. **69**, 305 (1982).
[26] G. Artioli, J. V. Smith, and Å. Kvick, Acta Crystallogr., Sect. C: Cryst. Struct. Commun. **40**, 1658 (1984).
[27] M. A. Spackman and H-P. Weber, J. Phys. Chem. **92**, 794 (1988).
[28] F. Stéphanie-Victoire and E. Cohen De Lara, J. Chem. Phys. **109**, 6469 (1998).
[29] C. M. B. Line and G. J. Kearley, Chem. Phys. **234**, 207 (1998).
[30] K. Hermansson and I. Olovsson, Theor. Chim. Acta **64**, 265 (1984).
[31] S-B. Zhu, S. Singh, and G. W. Robinson, J. Chem. Phys. **95**, 2791 (1991).
[32] R. Kahn, E. Cohen De Lara, and K. D. Möller, J. Chem. Phys. **83**, 2653 (1985).
[33] A. Wallqvist and B. J. Berne, J. Phys. Chem. **97**, 13841 (1993).
[34] C. H. Cho, S. Singh, and G. W. Robinson, J. Chem. Phys. **107**, 7979 (1997).
[35] P. Demontis, G. B. Suffritti, S. Bordiga, and R. Buzzoni, J. Chem. Soc., Faraday Trans. **91**, 525 (1995).
[36] D. Wolf, P. Keblinki, S. R. Phillpot, and J. Eggebrecht, J. Chem. Phys. **110**, 8254 (1999).
[37] W. C. Swope, H. C. Andersen, P. H. Berens, and K. R. Wilson, J. Chem. Phys. **76**, 637 (1982).
[38] P. Demontis and G. B. Suffritti, in *Modelling of Structure and Reactivity in Zeolites*, edited by C. R. A. Catlow (Academic, London, 1992).
[39] S. Kirkpatrick, C. D. Gelatt, Jr., and M. P. Vecchi, Science **220**, 671 (1983).
[40] D. van der Spoel, P. J. van Maarenand, and H. C. Berendsen, J. Chem. Phys. **108**, 10220 (1998).
[41] W. E. Thiessen and A. M. Narten, J. Chem. Phys. **77**, 2656 (1982).
[42] A. K. Soper, Chem. Phys. **107**, 61 (1986).
[43] K. Krynicki, C. D. Green, and D. Sawyer, Faraday Discuss. Chem. Soc. **66**, 199 (1978).
[44] A. K. Soper and M. G. Phillips, Chem. Phys. **107**, 47 (1986).
[45] G. E. Walrafen, J. Chem. Phys. **40**, 3249 (1964).
[46] A. N. Rusk, D. Williams, and M. R. Querry, J. Opt. Soc. Am. **61**, 895 (1971).
[47] M. N. Afsar and J. B. Hasted, J. Opt. Soc. Am. **67**, 902 (1977).
[48] J. B. Hasted, S. K. Husain, F. A. M. Frescura, and J. R. Birch, Chem. Phys. Lett. **118**, 622 (1985).
[49] V. M. Zolotarev and A. V. Demin, Opt. Spectrosc. **43**, 157 (1977) [Opt. Spektrosk. **43**, 271 (1977)].
[50] L. M. Sesé, Mol. Phys. **76**, 1335 (1992).
[51] L. Ojamäe, K. Hermansson, and M. Probst, Chem. Phys. Lett. **191**, 500 (1992).
[52] D. Marx and M. Parrinello, J. Chem. Phys. **104**, 4077 (1996).
[53] E. M. Tuckerman, D. Marx, M. L. Klein, and M. Parrinello, J. Chem. Phys. **104**, 5579 (1996).
[54] J. A. Odutola and T. R. Dyke, J. Chem. Phys. **72**, 5062 (1980).
[55] T. R. Dyke, K. M. Mack, and J. S. Muenter, J. Chem. Phys. **66**, 498 (1977).
[56] M. J. Wójcik and S. A. Rice, J. Chem. Phys. **84**, 3042 (1986).
[57] J.-R. Hill, C. L. Freeman, and B. Delley, J. Phys. Chem. **103**, 3772 (1999).
[58] B. Thimme Gowda and S. W. Benson, J. Chem. Phys. **79**, 1235 (1983).
[59] C. P. Schulz, R. Haugstätter, H. U. Tittes, and I. V. Hertel, Z. Phys. D: At., Mol. Clusters **10**, 279 (1988).
[60] I. V. Hertel, C. Huglin, C. Nitsch, and C. P. Schulz, Phys. Rev. Lett. **67**, 1767 (1991).
[61] X. Periole, D. Allouche, J.-P. Dadey, and Y.-H. Sanejouand, J. Phys. Chem. B **101**, 5018 (1997).
[62] E. D. Glendeling and D. Feller, J. Phys. Chem. **99**, 3060 (1995).
[63] B. Roux and M. Karplus, J. Comput. Chem. **16**, 690 (1995).
[64] C. W. Bauschlincher, S. R. Langhoff, H. Partrige, J. E. Rice, and A. Komornicki, J. Chem. Phys. **95**, 5142 (1991).
[65] R. N. Barnett and U. Landman, Phys. Rev. Lett. **70**, 1775 (1993).
[66] L. M. Ramaniah, M. Bernasconi, and M. Parrinello, J. Chem. Phys. **109**, 6839 (1998).
[67] W. L. Jorgensen, J. Chandrasekhar, J. D. Madura, R. W. Impey, and M. L. Klein, J. Chem. Phys. **79**, 926 (1983).
[68] P. Bopp, W. Dietz, and K. Heinzinger, Z. Naturforsch. A **34**, 1424 (1979).
[69] G. C. Lie and E. Clementi, Phys. Rev. A **33**, 2679 (1986).
[70] L. A. Curtiss, D. J. Frurip, and M. Blander, J. Chem. Phys. **71**, 2703 (1979).
[71] H. J. C. Berendsen, J. R. Grigera, and T. P. Straatsma, J. Phys. Chem. **91**, 6269 (1987).
[72] B. H. Torrie, I. D. Brown, and H. E. Petch, Can. J. Phys. **74**, 4872 (1981).